Available online at www.sciencedirect.com
SciVerse ScienceDirect
Ceramics International 39 (2013) 4679–4682
CERAMICS INTERNATIONAL
www.elsevier.com/locate/ceramint

Short communication

$La_{0.1}Bi_{0.9}FeO_3$–$BiY_2Fe_5O_{12}$ composites with simultaneously improved magnetization and polarization

Ying Lin, Haibo Yang*, Zhenfeng Zhu, Fen Wang

Key Laboratory of Auxiliary Chemistry & Technology for Light Chemical Industry, Ministry of Education, Shaanxi University of Science and Technology, Xi'an 710021, China

Received 27 September 2012; received in revised form 28 October 2012; accepted 28 October 2012
Available online 5 November 2012

Abstract

$La_{0.1}Bi_{0.9}FeO_3$–$BiY_2Fe_5O_{12}$ (LBFO–BYIG) composites were fabricated via a modified solid-sate method by mixing the LBFO powder into BYIG solution and then sintering. The phase compositions, magnetic and electrical properties of the composites were investigated. The results show that the LBFO and BYIG phases can coexist in the composite without any secondary phase. Compared to the weak magnetic and ferroelectric properties of LBFO, the magnetization and polarization of LBFO can be simultaneously improved by the introduction of BYIG phase due to the high magnetization and resistivity of BYIG. The coercivity is reduced by the introduction of BYIG, due to the ferrimagnetic nature of BYIG.

Keywords: B. Composites; C. Ferroelectric properties; C. Magnetic properties

1. Introduction

Multiferroic materials have been receiving continuous attention due to their technological significance and scientific value promised for several types of novel multifunctional devices, such as in memories, transducers, sensors, and spintronics [1–3]. More recently, the surge in interest has been further stimulated by the behavior of the unique room-temperature single-phase multiferroic $BiFeO_3$ (BFO) with high Curie ($T_C \sim 1103$ K) and Neel ($T_N \sim 643$ K) temperatures [4]. Whereas, its large leakage current at room temperature (RT) and weak magnetic behavior hinder the potentially feasible applications due to the presence of Fe^{2+} and oxygen vacancies and its spiral modulated spin structure, respectively [5,6]. Consequently, many approaches, such as chemical substitution [7,8] and formation of a multilayered structure [9,10], have been employed to improve the ferroelectric and magnetic properties, especially for BFO thin films. However, although slightly enhanced magnetization can be observed in highly constrained epitaxial films or chemically substituted films and bulks, the enhancement of magnetization is limited because they can only suppress or destroy the spin cycloid but cannot change the intrinsic antiferroelectric nature of BFO-based single-phase materials. Moreover, the excellent ferroelectric properties can be obtained for BFO thin films but the ferroelectric properties of BFO bulks are still not satisfactory. An alternative effective way of enhancing the magnetism for BFO-based multiferroics is to introduce suitable ferrites to form composites. Some previous studies [11] introduced $CoFe_2O_4$ ferrite to form BFO-based composite in order to increase the magnetization but the ferroelectric properties would be deteriorated owing to the low resistivity of $CoFe_2O_4$. Although single enhancement of magnetic or ferroelectric property has been achieved in many investigations on BFO bulks, the reports on the simultaneously enhanced magnetization and polarization of BFO bulks are scarce. $Y_3Fe_5O_{12}$ is a classical microwave ferrite with high magnetization and very high resistivity and its sintering temperature can be reduced from ~ 1400 °C to ~ 1000 °C by substitution of Bi^{3+} for Y^{3+} [12].

In the present work, $BiY_2Fe_5O_{12}$ (BYIG) was introduced into $La_{0.1}Bi_{0.9}FeO_3$ (LBFO) to form LBFO–BYIG composites. The magnetization and polarization of LBFO are improved simultaneously due to the high magnetization and resistivity of BYIG.

---

*Corresponding author.
E-mail address: yanghaibo@sust.edu.cn (H. Yang).

0272-8842/$ - see front matter © 2012 Elsevier Ltd and Techna Group S.r.l. All rights reserved.
http://dx.doi.org/10.1016/j.ceramint.2012.10.257

2. Experimental

The LBFO–BYIG composites were prepared by a modified solid-state method. Commercial La_2O_3, Bi_2O_3 and Fe_2O_3 were mixed thoroughly and calcined at 800 °C in air for 4 h. The calcined LBFO powders were milled into micrometer-size powders. Meanwhile, a BYIG sol was prepared according to the process of Reference [13]. All the above starting materials were from Sigma-Aldrich Pte. Ltd., Singapore and their purities were all above 99%. The micrometer LBFO powders were added into the BYIG sol with different mass ratios. After thoroughly mixing by ball milling, the obtained ceramic slurry was heated at 80 °C, 200 °C and 400 °C for 2 h, respectively, and then pressed into discs after adding proper amount of 5 wt% PVA solution. Final sintering was carried out at 900–1000 °C in air for 2 h. The phase composition of the LBFO–BYIG composites was analyzed by using an X-ray diffractometer (Bruker D8 Advanced XRD, Bruker AXS Inc., Madison, WI, Cu K). An impedance analyzer (Solartron grain phase analyzer) was employed to characterize the impedance properties of the composites. The ferroelectric properties of the composites were studied by using the Radiant precise workstation (Radiant Technologies, Medina, NY). The magnetic hysteresis loops of the composites were measured by a vibrating sample magnetometer 113 (VSM, Lake Shore 7410, Westerville, OH).

3. Results and discussion

The XRD patterns of the LBFO composites with different BYIG concentrations are shown in Fig. 1. It can be found that all the diffraction peaks of the composites can indexed to the desirable BFO–BT and BYIG phases and no any other phase can be detected, which indicates that the two phases can coexist in the composites and display wanted chemical compatibility. Moreover, as expected, the intensities of the diffraction peaks of BYIG phase increase with increasing the BYIG concentrations.

Fig. 2 shows the magnetic hysteresis loops (*M*–*H*) of the LBFO–BYIG composites with different BYIG concentrations. Obviously, the *M*–*H* loop of the pure LBFO is very slim, indicating its weak magnetism due to the antiferromagnetic nature. The striking result of Fig. 2 is that all the composites show obviously enhanced ferromagnetic properties and the magnetic properties are strongly dependent on BYIG concentrations. Compared with the magnetic properties of the pure LBFO, the saturated magnetization (M_s) of the composites is significantly enhanced and the coercivity is reduced by the introduction of BYIG, due to the ferrimagnetic nature of BYIG [14].

To elucidate the role of BYIG on the resistivity, the impedance of the composites has been measured. The complex impedance plot of the LBFO–BYIG composites with different BYIG concentrations is illustrated in Fig. 3. It can be seen that for all the composites each impedance

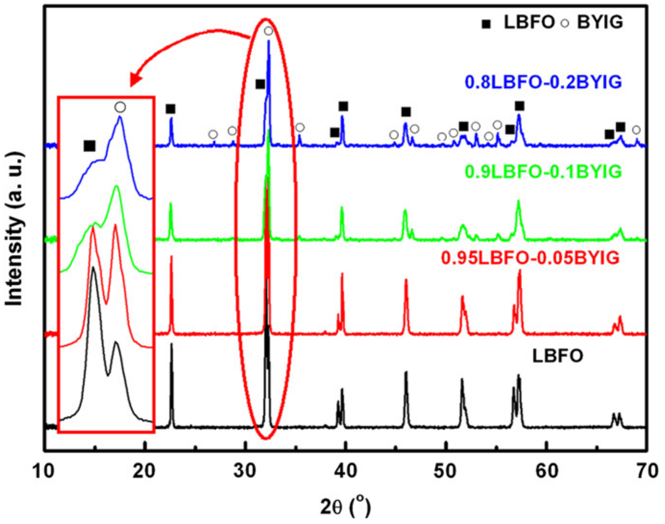

Fig. 1. XRD patterns of the LBFO–BYIG composites with different BYIG concentrations, where the inset is the magnification image of the peaks in the vicinity of 32°.

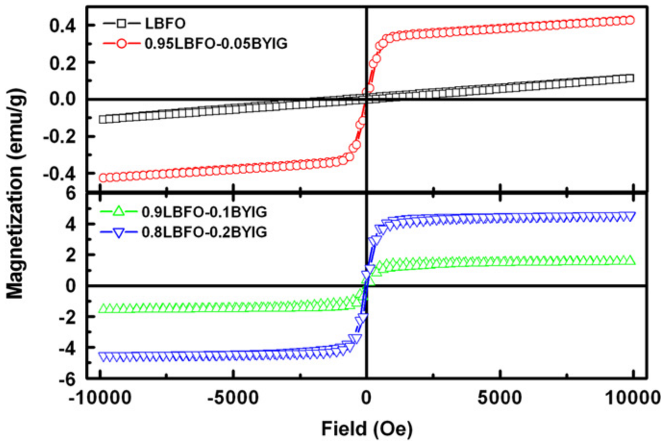

Fig. 2. Magnetic hysteresis (*M*–*H*) loops of the LBFO–BYIG composites.

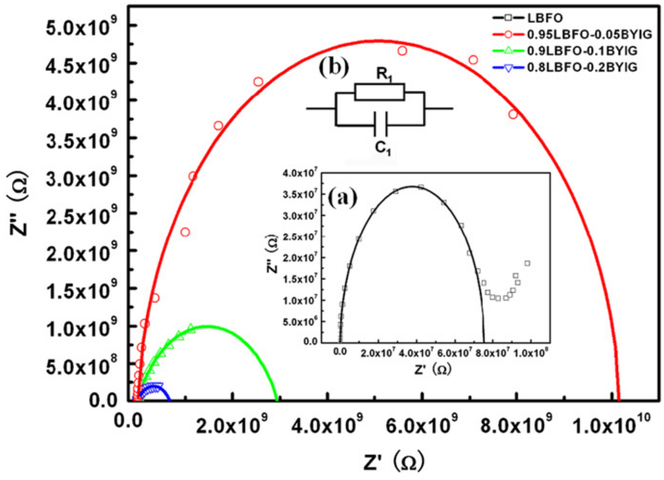

Fig. 3. Complex impedance plot of the LBFO–BYIG composites where the inset (a) is the complex impedance plot of the pure LBFO and the inset (b) is the equivalent circuit.

spectrum is a segment of arc. To analyze the impedance spectra, the results can be approximately modeled by an ideal equivalent circuit consisting of a resistor R and a capacitor C in parallel. For the pure LBFO, the *R* value is $7.5\times10^{7}\ \Omega$.

The *R* values are $1.01\times10^{10}\ \Omega$, $2.9\times10^{9}\ \Omega$, $6.6\times10^{8}\ \Omega$, respectively, as the BYIG concentrations ranging from 0.05 to 0.2, indicating that the *R* values of the composites are all high than that of pure LBFO and especially the *R* value of the 0.95LBFO–0.05BYIG composite is about 130 times higher than that of the pure LBFO. However, with further increasing the BYIG concentrations the *R* value decreases because of the deterioration of sintering density due to the shrinkage mismatch of the two phases, which can be evidenced by the SEM micrographs (not shown) of the surface of the composites.

Fig. 4 shows ferroelectric polarization hysteresis (*P–E*) loops of the LBFO–BYIG composites with different BYIG concentrations. For the pure LBFO, the *P–E* loop is very round due to very high leakage current and the sample is in the vicinity of breakdown at the electrical field strength of 10 kV/cm. The satisfactory result is that the composites show typical *P–E* loops, presenting a marked contrast with that of the pure LBFO. This phenomenon is due to the increased resistivities caused by the introduction of high resistive BYIG phase. It is worth noting that the remnant polarizations (P_r) of the LBFO–BYIG composites are all much larger than that of the pure LBFO. Among the LBFO–BYIG composites, the 0.95LBFO–0.05BYIG composite possesses the most resistive *P–E* loop at the highest electric field strength of 65 kV/cm. It can be also found that the coercive electric strength (E_c) of the 0.95LBFO–0.05BYIG composite is much higher than those of the other composites due to the fact that for the resistive 0.95LBFO–0.05BYIG composite more polarizations generated under higher electric strength and higher reverse electric strength, i.e. E_c, is needed to depolarize them. And the *P–E* loops become a little round again with further increasing the BYIG concentrations, which is consistent with the above impedance results.

4. Conclusions

In summary, the LBFO–BYIG composites were synthesized via a modified solid-sate method. The LBFO and BYIG phases can coexist in the composites without any secondary phase. Compared to the weak magnetic and ferroelectric properties of the pure LBFO, the magnetization and polarization can be simultaneously improved by the introduction of BYIG phase due to its higher magnetization and resistivity while the fact is reverse for the coercivity. The M_s of the composites increases with increasing the BYIG concentrations. The 0.95LBFO–0.05BYIG composite possesses the most resistive *P–E* loop at the highest electrical field strength of 65 kV/cm, and the *P–E* loops become a little round again with further increasing BYIG concentrations, which is

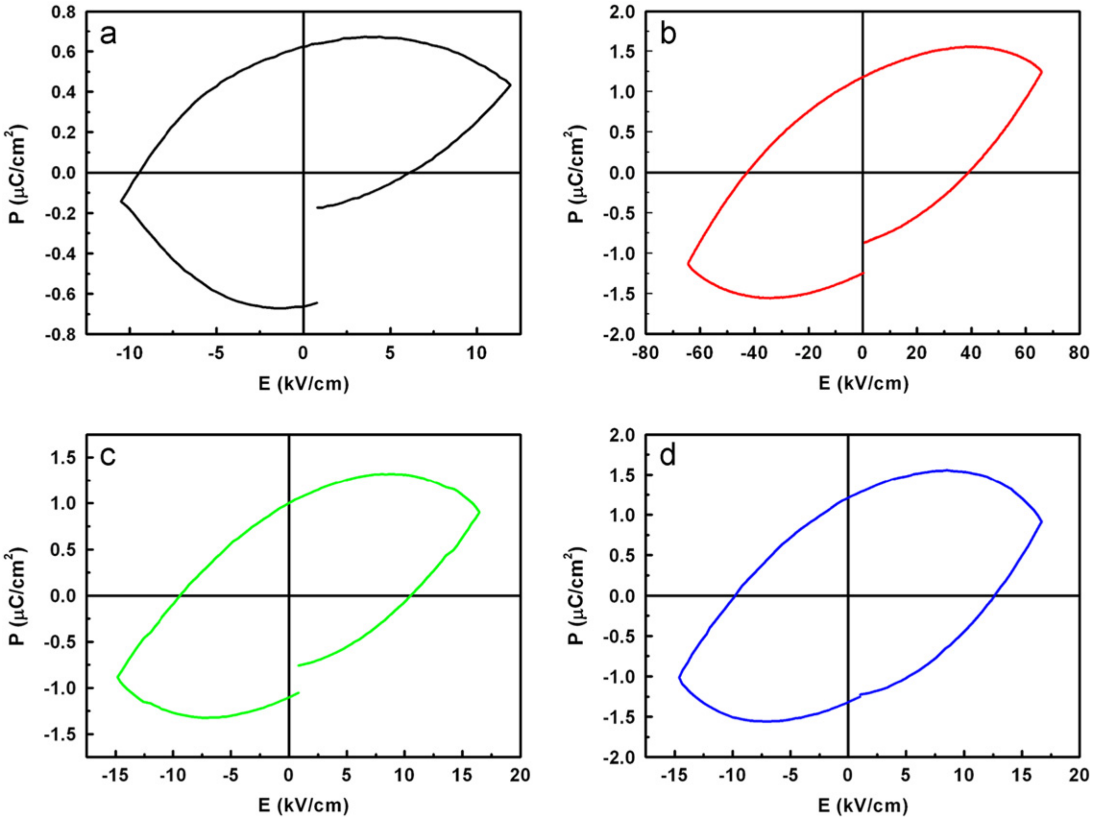

Fig. 4. Polarization hysteresis (*P–E*) loops of the BYIG composites: (a) pure LBFO; (b) 0.95LBFO–0.05BYIG; (c) 0.9LBFO–0.1BYIG; and (d) 0.8LBFO–0.2BYIG.

consistent with the impedance results, because of the deterioration of sintering density due to the shrinkage mismatch of the two phases.

Acknowledgments

This work is supported by the Natural Science Foundation of China (Grant no. 50902090), the Special Foundation of Educational Department of Shaanxi Province (Grant no. 11JK0823), and the Academic Backbone Cultivation Program of Shannxi University of Science and Technology (Grant no. XSG2010004).

References

[1] J. Ma, J.M. Hu, Z. Li, C.W. Nan, Recent progress in multiferroic magnetoelectric composites: from bulk to thin films, Advanced Materials 23 (2011) 1062–1087.

[2] C.W. Nan, M.I. Bichurin, S.X. Dong, D. Viehland, G. Srinivasan, Multiferroic magnetoelectric composites: historical perspective, status, and future directions, Journal of Applied Physics 103 (2008) 031101.

[3] Z.H. Dai, Y. Akishige, $BiFeO_3$ ceramics synthesized by spark plasma sintering, Ceramics International 38 (2012) S403–S406.

[4] J. Wang, J.B. Neaton, H. Zheng, V. Nagarajan, S.B. Ogale, B. Liu, D. Viehland, V. Vaithyanathan, D.G. Schlom, U.V. Waghmare, N.A. Spaldin, K.M. Rabe, M. Wuttig, R. Ramesh, Epitaxial $BiFeO_3$ multiferroic thin film heterostructures, Science 299 (2003) 1719.

[5] S.Y. Wang, X. Qiu, J. Gao, Y. Feng, W.N. Su, J.X. Zheng, D.S. Yu, D.J. Li, Electrical reliability and leakage mechanisms in highly resistive multiferroic $La_{0.1}Bi_{0.9}FeO_3$ ceramics, Applied Physics Letters 98 (2011) 152902.

[6] F. Yan, S. Miao, I. Sterianou, I.M. Reaney, M.O. Lai, L. Lua, W.D. Song, Multiferroic properties and temperature-dependent leakage mechanism of Sc-substituted bismuth ferrite–lead titanate thin films, Scripta Materialia 64 (2011) 458–461.

[7] N.M. Murari, R. Thomas, R.E. Melgarejo, S.P. Pavunny, R.S. Katiyar, Structural, electrical, and magnetic properties of chemical solution deposited $BiFe_{1-x}Ti_xO_3$ and $BiFe_{0.9}Ti_{0.05}Co_{0.05}O_3$ thin films, Journal of Applied Physics 106 (2009) 014103.

[8] B.C. Luo, C.L. Chen, Z. Xu, Q. Xie, Effect of Cr substitution on the multiferroic properties of $BiFe_{1-x}Cr_xO_3$ compounds, Physics Letters A 374 (2010) 4265–4268.

[9] J.G. Wu, J. Wang, Multiferroic behavior and impedance spectroscopy of bilayered $BiFeO_3/CoFe_2O_4$ thin films, Journal of Applied Physics 105 (2009) 124107.

[10] J.G. Wu, J. Wang, D.Q. Xiao, J.G. Zhu, Multiferroic and fatigue behavior of silicon-based bismuth ferrite sandwiched structure, Journal of Materials Chemistry 21 (2011) 7308–7313.

[11] X.H. Liu, Z. Xu, X.Y. Wei, Z.H. Dai, X. Yao, Ferroelectric, ferromagnetic, and magnetoelectric characteristics of $0.9(0.7BiFeO_3–0.3BaTiO_3)–0.1CoFe_2O_4$ ceramic composite, Journal of the American Ceramic Society 93 (2010) 2975–2977.

[12] H.J. Zhao, J. Zhou, B. Li, Z.L. Gui, L.T. Li, Microstructure and densification mechanism of low temperature sintering Bi-substituted yttrium iron garnet, Journal of Electroceramics 21 (2008) 802–804.

[13] T.T. Tsuchiya, T. Sei, H. Kanda, Sol–gel preparation of YIG ($Y_3F_5O_{12}$) thin film showing opto–magnetic effect, Journal of Non-Crystalline Solids 147–148 (1992) 463–466.

[14] E.J. Donahue, M. Ng, P. Li, A determination of structural evolution during the processing of glycol-based, sol–gel derived ceramics through the study of ferrimagnetic interactions, Journal of Materials Research 22 (2007) 3152–3157.